Published in final edited form as:
Cancer Res. 2011 April 1; 71(7): 2433–2444. doi:10.1158/0008-5472.CAN-10-1875.

Integration of Genotypic and Phenotypic Screening Reveals Molecular Mediators of Melanoma-Stromal Interaction

Megan J. Stine[1,2], **C. Joanne Wang**[3,4], **Whei F. Moriarty**[1,2], **Byungwoo Ryu**[1,6], **Raymond Cheong**[3,4], **William H. Westra**[5], **Andre Levchenko**[3,4], and **Rhoda M. Alani**[1,2,7]

[1] The Sidney Kimmel Comprehensive Cancer Center at Johns Hopkins, The Johns Hopkins University School of Medicine, 1650 Orleans Street, Baltimore, MD 21231-1000

[2] Program in Cellular and Molecular Medicine, The Johns Hopkins University School of Medicine, 1650 Orleans Street, Baltimore, MD 21231-1000

[3] Department of Biomedical Engineering, Whitaker Institute for Biomedical Engineering, The Johns Hopkins University School of Medicine, 1650 Orleans Street, Baltimore, MD 21231-1000

[4] Institute for Cellular Engineering, The Johns Hopkins University School of Medicine, 1650 Orleans Street, Baltimore, MD 21231-1000

[5] Department of Pathology, The Johns Hopkins University School of Medicine, 1650 Orleans Street, Baltimore, MD 21231-1000

Abstract

Tumor-endothelium interactions are critical for tumor survival and metastasis. Melanomas can rapidly metastasize early in tumor progression, but the dependence of this aggressive behavior on tumor-stromal interaction is poorly understood. To probe the mechanisms involved, we developed a heterotypic co-culture methodology, allowing simultaneous tracking of genomic and phenotypic changes in interacting tumor and endothelial cells in vitro. We found a dramatic re-arrangement of endothelial cell networks into patterns reminiscent of vascular beds, even on plastic and glass. Multiple genes were up-regulated in the process, many coding for cell surface and secreted proteins, including Neuropilin-2 (NRP2). A critical role of NRP2 in coordinated cell patterning and growth was confirmed using the co-culture system. We conclude that NRP2 represents an important mediator of melanoma-endothelial interactions. Furthermore, the described methodology represents a powerful yet simple system to elucidate heterotypic intercellular interactions mediating diverse physiological and pathological processes.

Introduction

Tumor metastasis is the cause of >90% of solid tumor deaths (1). Metastatic disease is particularly onerous in melanoma where the average life expectancy of patients with advanced disease is 6–9 months (2). In order for metastasis to occur, cells must dissociate from the primary tumor, locate and intravasate into a blood vessel, adhere to and extravasate

Correspondence to: Andre Levchenko; Rhoda M. Alani.

[6]Current address: Nevada Cancer Institute, One Breakthrough Way, Las Vegas, NV 89135

[7]Current address: Department of Dermatology, Boston University School of Medicine, 609 Albany Street, Suite J-507, Boston, MA 02118.

Author Contributions

The author(s) have made the following declarations about their contributions: Conceived and designed the experiments: MJS CJW WFM AL RMA. Performed the experiments: MJS CJW WFM BR WHW. Analyzed the data: MJS CJW WFM BR WHW RC AL RMA. Prepared the figures: MJS CJW WFM WHW BR RC. Wrote the paper: MJS CJW AL RMA.

from the vessel, adapt to a new microenvironment and undergo mitosis to form a new tumor at the secondary site (3,4). Recently, cell communication networks between a tumor and its surrounding microenvironment have garnered much attention, with mounting evidence supporting a critical role in the process of metastasis (reviewed in (5–7)). Over the past decade *in vivo* and *in vitro* model systems have been developed to better assess these particular communication networks (8–10); however, we still lack complete knowledge of the molecular mechanisms underlying tumor-stromal interactions. These molecular events are particularly consequential to cancers known to be “aggressive” such as melanoma (11). A critical hindrance to defining these molecular pathways is the paucity of simple, precise, and scalable methodologies allowing analysis of cell-cell communication.

Recent advances in microfabrication-based techniques have dramatically enhanced the degree of control of the analysis of cell behavior, in general, and cell-cell communication, in particular. Intercellular signaling has been studied by patterning cell pairs (12) or heterotypic cell populations, using a variety of techniques, including micro-stencils, microcontact cell printing, dielectrophoretic cell capture and reconfigurable micromechanic manipulation (13–15). These studies have led to interesting insights into the role of cellular communication in the control of a variety of biological processes, including angiogenesis, liver functioning and differentiation of various cell types. However, this type of experimentation is rarely combined with more conventional high throughput analysis of biochemical or genomic states of the interacting cells, e.g., microarray assay of alteration of gene expression programs.

In this report, we analyze the interaction between melanoma cells and endothelial cells in a series of well-controlled cell co-culture methods. A distinctive feature of this analysis is the ability to assess both the detailed phenotypes resulting from cell-cell communication, such as formation of cellular networks and cell migration and the large scale changes in gene expression engendered by tumor-endothelial cell-cell communication. This analysis has allowed us to identify a set of genes upregulated during *in vitro* melanoma-endothelial cell-cell communication, many of which have established roles in the control of angiogenesis. We furthermore provide evidence for the importance of neuropilin-2 (NRP2), one of the genes identified as upregulated in melanoma cells during co-culture, in the regulation of melanoma-endothelial inter-cellular communication through the control of patterned cell movement and the rate of melanoma cell division. These findings, as well as our ability to perform similar experiments with other tumor cell lines, support the general utility of this method for the analysis of varied instances of cell-cell communication involved in the formation of normal or malignant tissues, and may suggest new candidates for biomarkers of aggressive cancers.

Materials and Methods

Cell Culture

Melanoma cell lines were provided from the laboratory in which they originated by Meenhard Herlyn (Wistar Institute, Philadelphia, PA) and have been stored frozen as early-passage stocks for use in individual experiments. Cell lines have been well-characterized previously (16) and were tested for specific genetic mutations and authenticated as previously described (17) and cultured in DMEM with 10% FBS. Human Umbilical Vein Endothelial Cells (HUVEC) were purchased from Cambrex Bio Science Walkersville, Inc and cultured in EGM-2 (Lonza). HUVECs were discarded following passage 10. Additional tumor cell lines were obtained as gifts from various laboratories at Johns Hopkins University and are described in the Supplementary Materials and Methods. GFP and RFP labeling of cells was performed as previously described (18). All cell lines were passaged less than 6

months in culture after which time cells were re-initiated in culture from frozen stocks. Detailed cell culture protocols are provided in the Supplementary Materials and Methods.

Cell Tracking and Analysis of Cell Movement

The changes in the positions of individual HUVEC cells was manually tracked over time and the coordinates were recorded using custom-made software package implemented in Mathematica (version 6). The spatial correlation factor of the velocity vectors was calculated as a function of cell-cell distance *r* (not exceeding 200μm) in our analysis) for all cell pairs, as described previously (19):

$$C(r)=\sum_{i,j}^{r=|r_i-r_j|}\frac{(\vec{v}_i\cdot\vec{v}_j)}{|\vec{v}_i||\vec{v}_j|},$$

where v_i denotes the velocity vector of cell *i*, at position r_i, calculated from the difference between the cell positions in two images taken at an interval of 1 hour. When movement of a pair of cells is highly correlated, the value of *C(r)* can approach 1. Lower values of *C(r)* indicate lower correlation in the directional movement.

Cell Proliferation, TUNEL, and Scratch Assays

Cell proliferation XTT assays were performed using standard reagents (Cell Proliferation Kit II, Roche Applied Science). BrdU incorporation was measured using the BrdU Labeling and Detection Kit I (Roche Applied Science), following the manufacturer's instructions. TUNEL staining was performed using the In situ Cell Death Detection Kit, TMR Red (Roche Applied Science). Please refer to Supplementary Materials and Methods for detailed protocols.

Microarrays Data Analysis

Microarray analysis was performed as previously described (17). MIAME Compliance: All samples were run in commercial arrays from Affymetrix, using Affymetrix GeneChip human U133Plus 2.0 arrays as described by the manufacturer's instructions. The JHMI Microarray Core Facility abides in all its procedures by current MIAME guidelines. Microarray data has been submitted to the NCBI's Gene Expression Omnibus (GEO) repository under the series record GSE8699. Please refer to Supplementary Materials and Methods for detailed protocols.

Quantitative RT-PCR

The relative expression levels of VEGFR1, VEGFR2, and VEGFR3 in human melanoma cell lines and RFP-HUVECs were determined by quantitative real time polymerase chain reaction (qRT-PCR) analysis. Detailed protocols are provided in the Supplementary Materials and Methods.

Immunoblotting, Immunoprecipitations, Immunohistochemistry and Antibodies

Antibodies used included: NRP2 (sc-5542 and sc-13117, Santa Cruz), VEGFR2 (sc-504, Santa Cruz) and actin (sc-1616-R, Santa Cruz). For immunoprecipitations, protein extract was prepared using RIPA buffer with protease inhibitor cocktail (Sigma) and PMSF (Sigma). Please refer to Supplementary Materials and Methods for detailed protocols.

NRP2 shRNA knockdown

The lentiviral shRNA vectors pLKO.1 empty, pLKO.1 scrambled, and five pLKO.1 vectors targeting NRP2 were obtained from The RNA Interference Consortium shRNA library. Lipofectamine 2000 (Invitrogen) was used to transfect lentiviral shRNA as well as relevant helper plasmids into 293T cells. Viral supernatant collected from the transfection in addition with 8 μg/ml polybrene was used to infect 1205Lu cells. Cells were selected with 1 μg/mL puromycin.

Results

Melanoma-Endothelial Cell Communication is Observed *in vitro*

In order to define the putative molecular determinants of melanoma-endothelial cell communication, we designed systems for concurrent analysis of genotypic and phenotypic changes during cell co-culture. We explored three distinct *in vitro* two-dimensional co-culture systems of melanoma and endothelial cells (Figure 1A) which were designed to increase the degree of control of the co-culture and to easily distinguish constituent cells. First, we incubated adjacent colonies of melanoma and endothelial cells separated by a considerable distance (150–200 μm). The cells were then allowed to migrate and interact at the interface between colonies for 48 hrs, thus creating self-organizing cellular networks (method I, Figure 1A, left). In the second method, cells were pre-mixed at a 50/50 ratio, plated in this randomly mixed state and allowed to interact for the subsequent 48 hrs (method II, Figure 1A, middle). Finally, using stencil-based methodology, endothelial cells were patterned into circular or triangular shaped colonies of pre-defined size, with melanoma cells plated into the surrounding open spaces (method III, Figure 1A, right). The number of cells in each of the patterned colonies was controlled precisely (88 +/−14 cells for 1mm diameter circular colony; 72 +/−20 cells for 1mm-sided triangular colony). To distinguish melanoma and endothelial cells during and following co-incubation, we used the metastatic melanoma cell line, 1205Lu, carrying stably-integrated green fluorescent protein (GFP-1205Lu) and human umbilical vein endothelial cells stably transfected with red fluorescent protein (RFP-HUVECs). The three different co-incubation techniques employed primarily differ in terms of the nature and extent of the interface between heterotypic cells: the interface is initially absent but is emerging in the first method, it is very extensive but poorly controlled in the second method, and it is well defined and controlled but not very extensive in the third method. These differentially defined interfaces allow us to vary the extent of heterotypic cell interactions that might preferentially occur as a result of modulating their spatial relationship.

Using all three methods, we then examined the patterns of cell movement and colony organization over time. In method I, we observed striking emergence of endothelial cell networks as the tumor-endothelial cell interface gradually emerged and cells progressively intermingled (Figure 1B, bottom). Notably, these structures included continuous loops composed of endothelial cells that enclosed tumor cells and were of shape and form analogous to those seen in tumor parenchyma (20, 21). This structured assembly of endothelial cells differed from the random assembly observed with endothelial cells cultured alone (Figure 1F). Evaluation of random co-cultures of melanoma and endothelial cells, (method II), showed minimal HUVEC network formation at 6 hours of co-culture (Figure 1C, top), but pronounced cell network formation at 48 hours (Figure 1C, bottom). The networks formed by a gradual accumulation of endothelial cells into looped and branched structures distinguishable against the background of melanoma cells, with cell network morphology similar to that observed using method I. Using method III, we found that endothelial cells moved in collective migratory ‘streams’ out of the pre-patterned islands into the surrounding large scale colonies of melanoma cells, forming the initial branched

network (Figure 1D; Supplementary Movie 1). Thus, all three cell co-incubation methods resulted in an extensive reorganization of endothelial cells into branched and looped networks at the interfaces between heterotypic cell colonies. Importantly, this type of reorganization, suggesting formation of capillary-like cell networks, is usually observed in appropriate gel structures, rather than on plastic or glass, further hinting at a strong effect of co-culture.

We further sought to determine whether the observed cell patterning required direct cell-cell communication at the interfaces between heterotypic cell colonies, or could be mediated through secreted factors. We found that incubation of HUVECs in either basal medium alone or HUVEC-conditioned media for 48 hours failed to elicit HUVEC patterning *in vitro* (Figures 1E, 1F). However, incubation of HUVECs in either melanoma cell–conditioned media or co-culture-conditioned media induced cell re-organization into networks similar to those found using co-culture methods I and II at 48 hours of incubation (Figures 1G, 1H), suggesting that melanoma-HUVEC communication is mediated, at least in part, by one or more tumor-secreted soluble factor(s).

Differential Gene Expression during Melanoma-Endothelial Cell Communication

Since all three co-incubation methods used in the analysis resulted in progressively organizing networks of endothelial cells, we questioned whether these morphological changes were correlated with changes in the gene expression profiles within the cells. Among the co-culture methods used, method II is particularly advantageous for a large-scale evaluation in changes of genomic composition of cells participating in co-culture due to similar relative numbers of and an extensive interface between heterotypic cells. We took advantage of the nature of this system and the ability to sort heterotypic cells following co-culture using cell type-specific fluorescent labels to examine the gene expression profiles of sorted cells following co-culture. To define the molecular pathways governing melanoma-HUVEC communication, we performed gene expression profiling of GFP-1205Lu and RFP-HUVECs cultured alone or in mixture for 48 hrs (Figure 2A). Analysis of gene expression signatures associated with the co-culture system demonstrated specific influences of tumor cells on endothelial cell expression profiles and vice versa. Our initial analysis focused on the expression profile differences in melanoma cells. Evaluation of the Gene Ontology biological classifications of the genes upregulated in GFP-1205Lu cells following co-culture with HUVECs versus melanoma cells grown alone demonstrated alterations in genes controlling cell adhesion, cell migration, extracellular matrix organization, and angiogenesis, i.e., signatures frequently associated with tumor progression and metastasis (Table 1). Among the top 30 genes upregulated in melanoma cells under co-culture conditions were thymosin beta 4, a gene previously associated with tumor angiogenesis and melanoma metastasis (22–24), multimerin 1, a gene involved in endothelial cell adhesion (25), and Neuropilin-2 (NRP2) (Table 2). NRPs are transmembrane glycoproteins that modulate the development of the nervous and vascular systems (26–28). They function as co-receptors interacting with the vascular endothelial growth factor (VEGF) receptors and the plexins, and bind two known ligands with distinct functions: class 3 semaphorins, involved in axonal guidance; and VEGF family members known to promote angiogenesis. Blocking NRP2 function has recently been shown to inhibit tumor metastasis through effects on lymphendothelial cell migration and tumor-associated lymphangiogenesis (29). NRPs have also been implicated in tumorigenesis as they are expressed in a variety of cancers (26, 30–36). Additionally, NRP2 has recently been shown to regulate processes essential for melanoma metastasis and angiogenesis *in vivo* (34); however, the mechanism involved in this regulation is unclear. We therefore sought to evaluate the potential role of NRP2 in regulating the phenotypic cell responses to co-culture conditions observed using the various methods described above.

Neuropilin-2 is Upregulated During Melanoma-Endothelial Cell Communication and is Expressed in Metastatic Melanomas

NRP2 protein expression was evaluated in GFP-1205Lu melanoma cells during homotypic cell culture or following co-culture with RFP-HUVECs by immunoblotting, confirming co-culture increased expression of NRP2 in GFP-1205Lu (Figure 2B). Since we noted that HUVEC patterning was dependent on tumor-associated secreted soluble factors, and since NRP2 may exist in both a secreted form and as a cell surface receptor (28), we evaluated the expression of secretable NRP2 in conditioned media derived from either RFP-HUVECs alone, GFP-1205Lu cells alone, or from cells co-cultured using method II (Figure 2C). We found RFP-HUVECs alone can secret considerable amount of secreted NRP2, and furthermore, that GFP-1205Lu alone can produce low but detectable amounts of secreted NRP2. This raises the possibility that NRP2 could be produced by melanoma cells, at least partially, in soluble form, at levels that may be modulated by co-culture, thus being a potential putative mediator of paracrine melanoma-endothelial cell-cell communication. Indeed, the co-culture conditioned media showed significantly higher concentrations of NRP2 than either monolithic culture. Because our co-culture methods were developed to model melanoma metastasis, we sought to ensure that NRP2 would indeed be expressed in metastatic melanomas in vivo. Examination of NRP2 expression in primary human melanoma tissues demonstrated specific, high-level expression of NRP2 within the tumor parenchyma in 5/5 metastatic melanomas evaluated (Figure 2D-F); furthermore, such staining was consistent with tumor staining by the melanocyte marker, Melan-A (2G).

Neuropilin-2 Mediates Melanoma Cell Proliferation

Since NRP2 can interact with VEGF signaling known to regulate both cell proliferation and migration, we investigated the functional significance of NRP2 over-expression in melanoma-endothelial co-cultures using an NRP2-neutralizing antibody (37,38). Interestingly, even in the absence of co-culture, we found that an NRP2-neutralizing antibody severely decreased melanoma cell growth *in vitro* (Figure 3A) suggesting that NRP2 is a critical mediator of melanoma cell proliferation. Studies with an alternative NRP2-neutralizing antibody also confirmed a growth inhibitory role (Figure S1) and BrdU incorporation assays demonstrated significant growth inhibition at 48 hours following antibody treatment (Figure 3D). Growth inhibition was titratable, as decreasing amounts of antibody had less of an inhibitory effect (Figure 3A–C). NRP2 knockdown in 1205Lu cells also showed growth inhibition of melanoma cells (Figure 3E–F). We note that previously, a modeling analysis indicated that the effects of neuropilin knockdown and Ab-mediated inhibition of neuropilin-VEGFR coupling might be very different, favoring Ab-mediated perturbation for therapeutic purposes (39). Evaluation of cellular apoptosis by TUNEL staining demonstrated no notable increase in melanoma cell death (Figure S2A–C). In addition, tumor cell morphology was not significantly altered following treatment with neutralizing antibody (Figure S2D, E). Furthermore, antibody neutralization of NRP2 did not significantly alter cell migration in a scratch assay when proliferation was taken into account (Figure S2F). These results suggest that NRP2 expressed by melanoma cells in homotypic cell culture specifically supports cell proliferation, possibly by facilitating autocrine signaling by VEGF (40).

NRP2 Promotes Collective Movement of HUVECs in Melanoma Co-Culture

We next turned to investigate whether NRP2 could also control directed endothelial cell migration into branched and looped networks observed with all co-culture methods using temporally resolved time-lapse imaging of HUVEC cell movement. For this purpose, the most controlled method of cell co-culture, method III, was employed due to the high degree of reproducibility of the initial conditions. Collective movement of endothelial cells was quantified by estimating the correlation of cell velocities for various cell pairs $C(r)$, as a

function of the distance between the cells (*r*) (as described in (19), see Methods for more details) for the control (HUVEC colony alone) and co-culture experiments at early (5 hours) and late (40 hours) time points (Figure 4, cf. Figs. 1A–III, 1D). Note that, although C(*r*) is expected to be 0 for sparse pure HUVEC colonies, it is commonly much higher for dense colonies, even in the absence of co-culture. This is in part due to correlated cell movement away from the center of the colony into available spaces for the distances measured (<200μm). We found that melanoma cells significantly enhanced directed HUVEC migration at the early but not at the late time point. Strikingly, NRP2-neutralizing antibody completely abolished this early enhancement effect by melanoma cells (Figure 4B, E), suggesting that NRP2 plays a critical role in mediating endothelial cell organization during the initial stages of the cellular network formation. Furthermore, the effect of the NRP2-neutralizing antibody was most pronounced at relatively large cell-cell distances (> 120 μm). These observations suggest that NRP2 effects on endothelial cell migration during co-culture are likely to be long range, and may influence cell behavior through a diffusion-based process rather than contact-based cell-cell interactions, in agreement with the results of the experiments with conditioned media. These results further imply that the branching patterns observed in heterotypic co-cultures (Figures 1B–D) may, at least in part, be dependent on the initial (over the first 5 hrs.), NRP2-dependent correlation in cell movement, direction, and speed.

NRP2 Receptors and Ligands are Expressed in Melanomas

To define the pathways associated with the NRP2 function in melanomas, we evaluated the expression of NRP2 ligands and co-receptors in a panel of melanoma cell lines. Previous gene expression studies of melanoma cell lines from varying stages of malignant progression allowed us to define the molecular signatures associated with melanoma progression (17). These data were mined to investigate expression of NRP2, its homologue NRP1, and its binding partners: VEGFR1, plexinA4A, plexinA3, VEGF-A, VEGF-C, and Sema3F. We detected NRP2 expression in all stages of melanoma with lower expression noted in 2 of 3 radial growth phases (Figure S3A). The expression of VEGF-A was elevated in early versus late stage melanomas (Figure S3A), while low-level expression of Plexins, Sema3F, and VEGF-C was seen in all melanoma cell lines evaluated and Nrp1 expression was virtually absent (Figure S3A). VEGF receptor expression was further evaluated by quantitative RT-PCR (Figure S3B). All cell lines examined expressed high levels of VEGFR1, with variable low-level VEGFR2 and VEGFR3 expression. NRP2 protein expression was also at the highest level in vertical growth phase melanomas, with little detectable protein in 2 of 3 of early (radial) growth phase melanomas (Figure S3C). These results suggested that NRP2 could exercise its effects through its natural binding partners, including, most notably, VEGF receptors.

Patterning Interactions between Tumor Cells and Endothelial Cells Varies with Tumor Type

We next evaluated the ability of various tumor cells to promote HUVEC patterning using co-culture method I (Figure 5). Patterning was assessed by quantifying the circular areas formed by networks of HUVEC cells using an automated image-analysis system (Figure 5A–C, bottom). Interestingly, we found a range of HUVEC pattern induction by various tumor cell lines with mild to moderate patterning induced by ovarian, colon, and pancreatic cancer cells, and the strongest patterning induced by non-small cell lung cancer, prostate cancer, breast cancer, glioblastoma, and melanoma cells (Figure 5D). Although there was not a strict correlation between tumor cell expression of NRP2 and patterning (Figure 5E), 3 of the top 5 patterning-associated tumor cell lines expressed significant levels of NRP2.

Discussion

Tumor growth and metastasis are complex processes that require intricate interactions with the surrounding stroma. One important consequence of these interactions is the extensive restructuring of endothelium adjacent to a developing tumor leading to tumor-associated angiogenesis. Another important consequence of such interactions is the ability of a tumor cell to breach an endothelial cell barrier in order to enter the vasculature, potentially resulting in metastasis. The mechanisms underlying angiogenesis and tumor metastasis are poorly understood due to their multifaceted and complex nature. To address these challenges, we took a reductionist approach to defining these systems by developing simple heterotypic cell co-culture methods to serve as *in vitro* models of tumor-stromal interactions that would allow detailed genotypic and phenotypic analysis and would facilitate tracking and sorting of participating cells. These analyses led to identification of multiple genes altered in melanoma cells during co-culture with HUVECs which are associated with the angiogenic phenotype, cellular migration, extracellular matrix remodeling, and cellular adhesion, suggesting that the described approach may be informative about the molecular alterations occurring during complex metastatic events *in vivo.* Indeed, previous investigations have remarked on the vasculogenic phenotype of advanced melanomas (41–44) which have been variously attributed to cell-autonomous angiogenic properties of melanoma cells themselves. Our current study suggests a more complex picture, according to which melanoma cells can be induced by neighboring endothelial cells to produce factors that can in turn influence endothelial cells, and their propensity to form functional vasculature.

A closer examination of the highly upregulated genes suggests that many of them code for secreted components that might be responsible for ensuring fast and robust formation of *de novo* vascular beds (12). Several of the highly upregulated genes identified have also been identified in reactive oxygen-driven tumors (44). This implicates the possibility of upregulation of reactive oxygen signaling in the co-culture system.

We have chosen to further evaluate NRP2 as a mediator of melanoma-endothelial cell communication and investigate its role in melanoma development and progression. Although NRP2 has been shown to be expressed in melanoma cell lines (31,33,45), its expression in primary human melanomas and its precise role in melanoma development and progression has not been delineated previously. We found NRP2 knockdown inhibited melanoma cell proliferation in addition to the specific and titratable inhibition of melanoma cell proliferation by an NRP2-neutralizing antibody, suggesting an important role of NRP2 in melanoma cell proliferation. It is notable that recently, semaphorins and VEGFs were shown to bind to distinct extracellular domains of NRP2 and that targeted antibodies can inhibit the binding of a specific ligand to NRP2 without influencing the binding of other ligands at other antigenic sites (46). The antibody evaluated in our studies was generated against amino acids 560–858 of NRP2 and would therefore block binding of both semaphorin and VEGF ligands. These results support a potentially critical role for VEGF and/or semaphorins in regulating melanoma cell growth in pure cultures or co-culture experiments; however the large numbers of interactions between NRPs, their co-receptors and numerous ligands suggest that the mechanisms of action of these antibodies is likely to be complex.

We also found a significant effect of NRP2-neutralizing antibody on HUVEC patterning induced by melanoma cells in co-culture due, at least in part, to reduced long-range coordination of cell movement at the initial stages of network formation. This suggests that NRP2, likely in its secreted form, assists melanoma cells in recruitment of endothelial cells towards the development of a functional new vasculature, thus enhancing melanoma

survival and providing potential routes for metastasis. The CM-induced cell patterning experiments further suggests that the interactions between NRP2 and its associated ligands and co-receptor are complex, and a delicate balance of their levels in the microenvironment is likely to be critical to the effects associated with cell patterning. The results also raises the possibility that post-translational modification of NRP2 within 1205Lu cells may be different from that within HUVECs, thus causing the variable effects of NRP2 in conditioned media from these two sources. NRP2 is notably polysialylated in dendritic cells (47); however, additional post-translational modifications is other cell types have not ben further elucidated to date. Clarification of the effects of NRP2 within the context of 1205Lu conditioned media would be interesting for further studies. Given the *in vivo* (29) and this *in vitro* evidence regarding NRP2 functions in melanoma growth and tumor metastasis, we conclude that NRP2 is an important mediator of melanoma-endothelial cell communication.

Our studies suggest that in addition to metastatic melanoma, glioblastoma cells express high levels of NRP2, which in turn may promote communication with and patterning of endothelial cells. It is striking that NRP2 functions at an interface of neural cell and endothelial cell fates, and that melanoma cells elicit such a strong response to communication with endothelial cells through this co-receptor. Much recent work has focused on this particular interface between neural and vascular circuitry (48–50). As melanoma is a malignant growth of the neural crest-derived melanocyte, the strong communication network of these tumor cells with their associated vasculature may display features of the developmental interactions between neural and endothelial cells. Indeed, it may be that the striking ability for melanomas to metastasize at early stages of development relates to their genetic memory of developmental cues associated with neural crest migration.

Finally, it is notable that the analyses of cell-cell communication used in this study may prove useful in exploring interactions between endothelial cells and other cancer cell types (Fig. 5), as well as other instances of intercellular signaling occurring *in vivo*. Indeed the correlation of phenotypic and genotypic changes accompanying cell-cell communication on the scale of interacting heterotypic cell populations remains poorly explored. The co-culture methods used here can help address whether the phenotypic changes engendered by cell-cell communication might depend on the nature and extent of the interface between interacting cell types. This analysis can be further extended to cover alterations in biochemical networks other than gene expression profiles. We thus anticipate that this method may become widely adopted as a means of discovery of novel factors controlling cell communication. We further suggest that such discovery efforts will lay the groundwork for identification of novel biomarkers and therapeutic targets for a variety of malignancies for which such communication networks are critical in tumor cell growth and metastasis.

Supplementary Material

Refer to Web version on PubMed Central for supplementary material.

Acknowledgments

We thank D. Ginty, J. Flook, K. Fritz, F. Murillo, C. C. Talbot, A. DeMarzo, J. Hicks, and C. Herrera for technical assistance and helpful advice. P. Cole, D. Ginty, and members of the Alani Lab for careful review of this manuscript and suggestions. This work was supported by grants from the National Cancer Institute CA107017 (RA), the Flight Attendant Medical Research Institute (RA), The American Skin Association (RA), the Institute for Cell Engineering (AL), The Joanna M. Nicolay Melanoma Foundation, The Murren Family Foundation, and The Henry and Elaine Kaufman Foundation.

Abbreviations

NRP2	neuropilin-2
VEGF	vascular endothelial growth factor
RFP-HUVEC	human umbilical vein endothelial cells stably-integrated with red fluorescent protein
GFP-1205Lu	metastatic melanoma cell line, 1205Lu, carrying stably-integrated green fluorescent protein

References

1. Gupta GP, Massague J. Cancer metastasis: building a framework. Cell. 2006; 127:679–695. [PubMed: 17110329]
2. Balch CM, Buzaid AC, Soong SJ, et al. Final version of the American Joint Committee on Cancer staging system for cutaneous melanoma. J Clin Oncol. 2001; 19:3635–3648. [PubMed: 11504745]
3. Fidler IJ. The pathogenesis of cancer metastasis: the ‘seed and soil’ hypothesis revisited. Nat Rev Cancer. 2003; 3:453–458. [PubMed: 12778135]
4. Nguyen DX, Massague J. Genetic determinants of cancer metastasis. Nat Rev Genet. 2007; 8:341–352. [PubMed: 17440531]
5. Liotta LA, Kohn EC. The microenvironment of the tumour-host interface. Nature. 2001; 411:375–379. [PubMed: 11357145]
6. Chambers AF, Groom AC, MacDonald IC. Dissemination and growth of cancer cells in metastatic sites. Nat Rev Cancer. 2002; 2:563–572. [PubMed: 12154349]
7. Kalluri R, Zeisberg M. Fibroblasts in cancer. Nat Rev Cancer. 2006; 6:392–401. [PubMed: 16572188]
8. Shioda T, Munn LL, Fenner MH, Jain RK, Isselbacher KJ. Early events of metastasis in the microcirculation involve changes in gene expression of cancer cells. Tracking mRNA levels of metastasizing cancer cells in the chick embryo chorioallantoic membrane. Am J Pathol. 1997; 150:2099–2112. [PubMed: 9176401]
9. Anderson AR, Weaver AM, Cummings PT, Quaranta V. Tumor morphology and phenotypic evolution driven by selective pressure from the microenvironment. Cell. 2006; 127:905–915. [PubMed: 17129778]
10. Bockhorn M, Jain RK, Munn LL. Active versus passive mechanisms in metastasis: do cancer cells crawl into vessels, or are they pushed? Lancet Oncol. 2007; 8:444–448. [PubMed: 17466902]
11. Fecher LA, Cummings SD, Keefe MJ, Alani RM. Toward a molecular classification of melanoma. J Clin Oncol. 2007; 25:1606–1620. [PubMed: 17443002]
12. Yin Z, Noren D, Wang CJ, Hang R, Levchenko A. Analysis of pairwise cell interactions using an integrated dielectrophoretic-microfluidic system. Mol Syst Biol. 2008; 4:232. [PubMed: 19096359]
13. Albrecht DR, Underhill GH, Wassermann TB, Sah RL, Bhatia SN. Probing the role of multicellular organization in three-dimensional microenvironments. Nat Methods. 2006; 3:369–375. [PubMed: 16628207]
14. Hui EE, Bhatia SN. Micromechanical control of cell-cell interactions. Proc Natl Acad Sci US A. 2007; 104:5722–5726.
15. Khetani SR, Bhatia SN. Microscale culture of human liver cells for drug development. Nat Biotechnol. 2008; 26:120–126. [PubMed: 18026090]
16. Satyamoorthy K, DeJesus E, Linnenbach AJ, et al. Melanoma cell lines from different stages of progression and their biological and molecular analyses. Melanoma Res. 1997; 7 (Suppl 2):S35–42. [PubMed: 9578415]
17. Ryu B, Kim DS, Deluca AM, Alani RM. Comprehensive expression profiling of tumor cell lines identifies molecular signatures of melanoma progression. PLoS One. 2007; 2:e594. [PubMed: 17611626]

18. Dunlap S, Yu X, Cheng L, Civin CI, Alani RM. High-efficiency stable gene transduction in primary human melanocytes using a lentiviral expression system. J Invest Dermatol. 2004; 122:549–551. [PubMed: 15009744]
19. Haga H, Irahara C, Kobayashi R, Nakagaki T, Kawabata K. Collective movement of epithelial cells on a collagen gel substrate. Biophys J. 2005; 88:2250–2256. [PubMed: 15596493]
20. Asaishi K, Endrich B, Gotz A, Messmer K. Quantitative analysis of microvascular structure and function in the amelanotic melanoma A-Mel-3. Cancer Res. 1981; 41:1898–1904. [PubMed: 7214358]
21. Endrich B, Hammersen F, Gotz A, Messmer K. Microcirculatory blood flow, capillary morphology and local oxygen pressure of the hamster amelanotic melanoma A-Mel-3. J Natl Cancer Inst. 1982; 68:475–485. [PubMed: 6950176]
22. Clark EA, Golub TR, Lander ES, Hynes RO. Genomic analysis of metastasis reveals an essential role for RhoC. Nature. 2000; 406:532–535. [PubMed: 10952316]
23. Ridley A. Molecular switches in metastasis. Nature. 2000; 406:466–467. [PubMed: 10952292]
24. Cha HJ, Jeong MJ, Kleinman HK. Role of thymosin beta4 in tumor metastasis and angiogenesis. J Natl Cancer Inst. 2003; 95:1674–1680. [PubMed: 14625258]
25. Adam F, Zheng S, Joshi N, et al. Analyses of cellular multimerin 1 receptors: in vitro evidence of binding mediated by alphaIIbbeta3 and alphavbeta3. Thromb Haemost. 2005; 94:1004–1011. [PubMed: 16363244]
26. Bielenberg DR, Pettaway CA, Takashima S, Klagsbrun M. Neuropilins in neoplasms: expression, regulation, and function. Exp Cell Res. 2006; 312:584–593. [PubMed: 16445911]
27. Favier B, Alam A, Barron P, et al. Neuropilin-2 interacts with VEGFR-2 and VEGFR-3 and promotes human endothelial cell survival and migration. Blood. 2006; 108:1243–1250. [PubMed: 16621967]
28. Staton CA, Kumar I, Reed MW, Brown NJ. Neuropilins in physiological and pathological angiogenesis. J Pathol. 2007; 212:237–248. [PubMed: 17503412]
29. Caunt M, Mak J, Liang WC, et al. Blocking neuropilin-2 function inhibits tumor cell metastasis. Cancer Cell. 2008; 13:331–342. [PubMed: 18394556]
30. Klagsbrun M, Takashima S, Mamluk R. The role of neuropilin in vascular and tumor biology. Adv Exp Med Biol. 2002; 515:33–48. [PubMed: 12613541]
31. Bielenberg DR, Hida Y, Shimizu A, et al. Semaphorin 3F, a chemorepulsant for endothelial cells, induces a poorly vascularized, encapsulated, nonmetastatic tumor phenotype. J Clin Invest. 2004; 114:1260–1271. [PubMed: 15520858]
32. Chen C, Li M, Chai H, Yang H, Fisher WE, Yao Q. Roles of neuropilins in neuronal development, angiogenesis, and cancers. World J Surg. 2005; 29:271–275. [PubMed: 15696396]
33. Chabbert-de Ponnat I, Buffard V, Leroy K, et al. Antiproliferative effect of semaphorin 3F on human melanoma cell lines. J Invest Dermatol. 2006; 126:2343–2345. [PubMed: 16691189]
34. Ellis LM. The role of neuropilins in cancer. Mol Cancer Ther. 2006; 5:1099–1107. [PubMed: 16731741]
35. Guttmann-Raviv N, Kessler O, Shraga-Heled N, Lange T, Herzog Y, Neufeld G. The neuropilins and their role in tumorigenesis and tumor progression. Cancer Lett. 2006; 231:1–11. [PubMed: 16356825]
36. Bielenberg DR, Klagsbrun M. Targeting endothelial and tumor cells with semaphorins. Cancer Metastasis Rev. 2007; 26:421–431. [PubMed: 17768598]
37. Nasarre P, Constantin B, Rouhaud L, et al. Semaphorin SEMA3F and VEGF have opposing effects on cell attachment and spreading. Neoplasia. 2003; 5:83–92. [PubMed: 12659673]
38. Nasarre P, Kusy S, Constantin B, et al. Semaphorin SEMA3F has a repulsing activity on breast cancer cells and inhibits E-cadherin-mediated cell adhesion. Neoplasia. 2005; 7:180–189. [PubMed: 15802023]
39. Mac Gabhann F, Popel AS. Targeting neuropilin-1 to inhibit VEGF signaling in cancer: Comparison of therapeutic approaches. PLoS Comput Biol. 2006; 2:e180. [PubMed: 17196035]

40. Graells J, Vinyals A, Figueras A, et al. Overproduction of VEGF concomitantly expressed with its receptors promotes growth and survival of melanoma cells through MAPK and PI3K signaling. J Invest Dermatol. 2004; 123:1151–1161. [PubMed: 15610528]
41. Hendrix MJ, Seftor EA, Hess AR, Seftor RE. Vasculogenic mimicry and tumour-cell plasticity: lessons from melanoma. Nat Rev Cancer. 2003; 3:411–421. [PubMed: 12778131]
42. Velazquez OC, Herlyn M. The vascular phenotype of melanoma metastasis. Clin Exp Metastasis. 2003; 20:229–235. [PubMed: 12741681]
43. Dome B, Hendrix MJ, Paku S, Tovari J, Timar J. Alternative vascularization mechanisms in cancer: Pathology and therapeutic implications. Am J Pathol. 2007; 170:1–15. [PubMed: 17200177]
44. Hess AR, Margaryan NV, Seftor EA, Hendrix MJ. Deciphering the signaling events that promote melanoma tumor cell vasculogenic mimicry and their link to embryonic vasculogenesis: role of the Eph receptors. Dev Dyn. 2007; 236:3283–3296. [PubMed: 17557303]
45. Lacal PM, Failla CM, Pagani E, et al. Human melanoma cells secrete and respond to placenta growth factor and vascular endothelial growth factor. J Invest Dermatol. 2000; 115:1000–1007. [PubMed: 11121133]
46. Appleton BA, Wu P, Maloney J, et al. Structural studies of neuropilin/antibody complexes provide insights into semaphorin and VEGF binding. Embo J. 2007; 26:4902–4912. [PubMed: 17989695]
47. Curreli S, Arany Z, Gerardy-Schahn R, Mann D, Stamatos NM. Polysialylated Neuropilin-2 Is Expressed on the Surface of Human Dendritic Cells and Modulates Dendritic Cell-T Lymphocyte Interactions. Journal of Biological Chemistry. 2007; 282:30346–30356. [PubMed: 17699524]
48. Carmeliet P, Tessier-Lavigne M. Common mechanisms of nerve and blood vessel wiring. Nature. 2005; 436:193–200. [PubMed: 16015319]
49. Suchting S, Bicknell R, Eichmann A. Neuronal clues to vascular guidance. Exp Cell Res. 2006; 312:668–675. [PubMed: 16330027]
50. Makita T, Sucov HM, Gariepy CE, Yanagisawa M, Ginty DD. Endothelins are vascular-derived axonal guidance cues for developing sympathetic neurons. Nature. 2008; 452:759–763. [PubMed: 18401410]

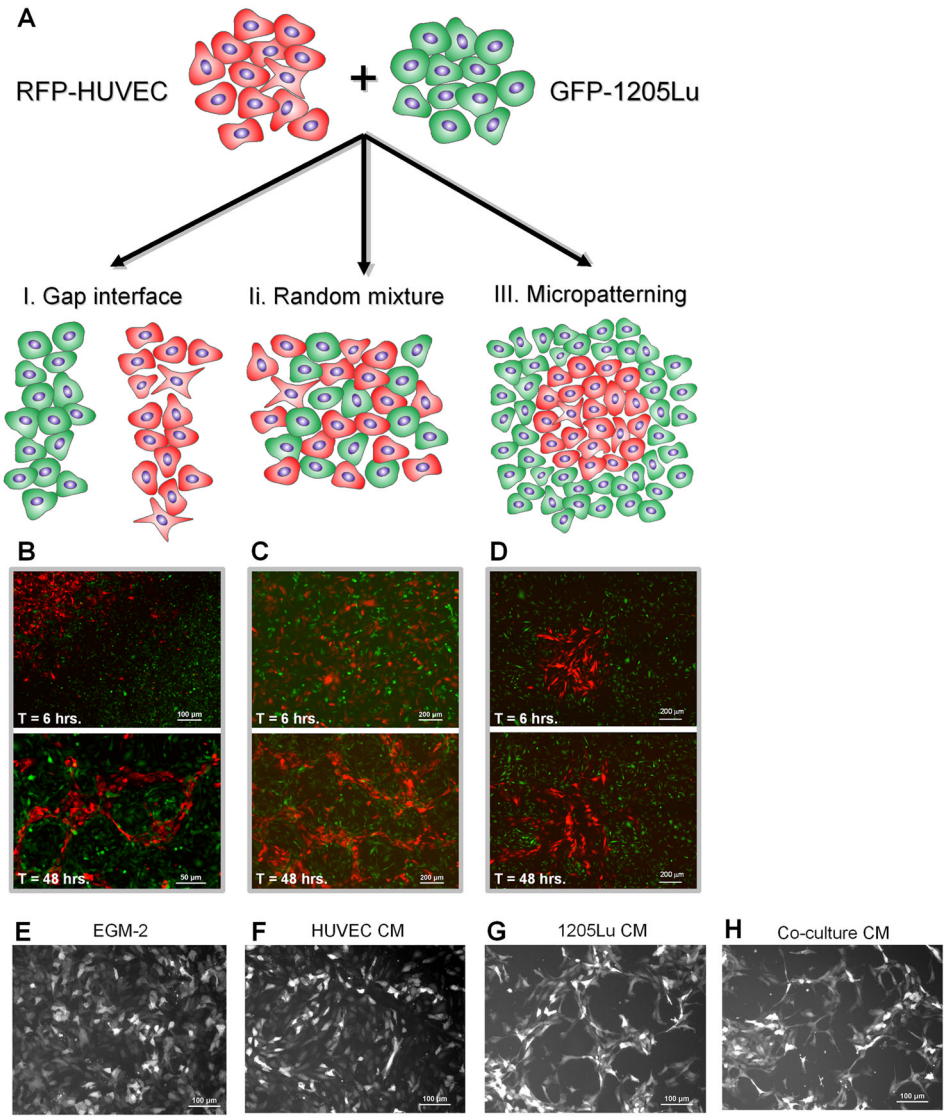

Figure 1. Methods of Controlled Heterotypic Cell Co-Culture Allow Analysis of the Cell-Cell Communication Phenotype

(A–D) RFP-HUVEC and GFP-1205Lu metastatic melanoma cells were co-cultured in colonies separated by a precisely defined gap (method I), in random mixtures (method II) or with an RFP-HUVEC colony of precisely defined size and shape surrounded by GFP-1205Lu cells (method III); the phenotypes of cells co-cultured using method I (B), method II (C) and method III (D) were determined at 6 hrs. (upper panels) and 48 hrs. (lower panel).

(E–H) RFP-HUVECs alone were cultured for 48 hrs. in EGM-2 medium (E) or in conditioned medium (CM) from HUVECs (F), 1205Lu cells (G), or co-cultured RFP-HUVEC and GFP-1205Lu cells (H).

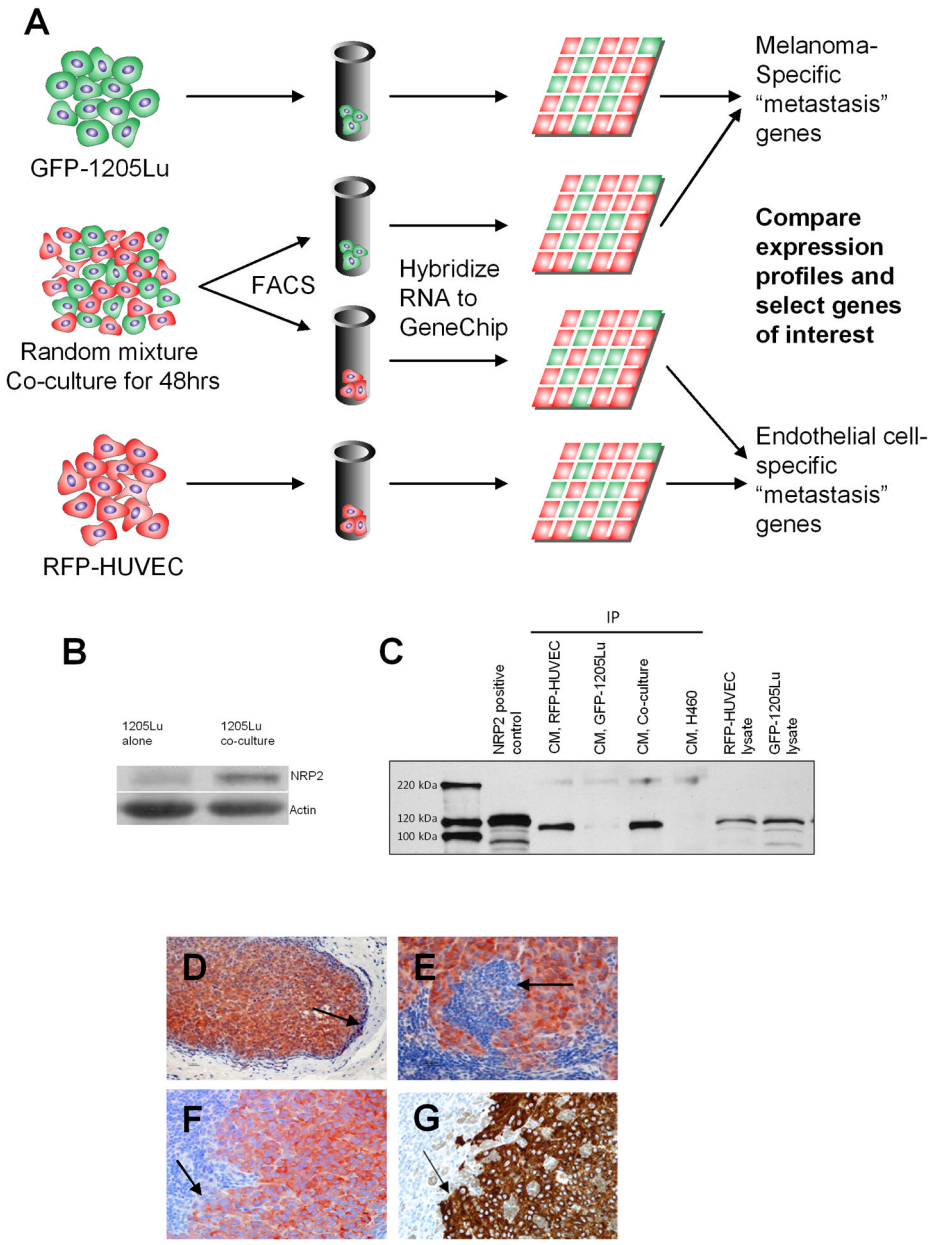

Figure 2. Global Gene Expression Profiling of Melanoma-Endothelial Cell Interactions Identifies Neuropilin-2 as A Mediator of Cellular Communication

(A) Schematic representation of screen to identify genes involved in melanoma-endothelial cell communication. Populations of RFP-HUVECs and GFP-1205Lu metastatic melanoma cells were plated in a co-culture system (method II) and incubated for 48 hours. Cells were sorted by FACS and RNAs isolated and hybridized to a pan-genomic human GeneChip. Expression profiles altered by co-culture were compared against those in homotypic cultures of RFP-HUVECs and GFP-1205Lu cells to identify genes associated with melanoma-endothelial cell communication.

(B) Western blot for NRP2 expression in GFP-1205Lu cells grown in homotypic cell culture or following heterotypic co-culture with RFP-HUVECs.

(C) IP-Western analysis of NRP2 expression in conditioned medium from RFP-HUVECs, GFP-1205Lu melanoma cells or HUVEC-1205Lu co-cultures. H460 (NRP1+/NRP2−) lung

cancer cells are included as a negative control for NRP2. RFP-HUVEC and GFP-1205Lu cell lysates are included as controls for non-secreted expression of NRP2.
(D–F) Immunohistochemical staining for NRP2 in human melanoma metastases at low-power magnification (D) and high-power magnification (E, F). Arrows point to demarcation of tumor-metastatic niche interface.
(G) Melan-A stain for melanoma cells depicted in (F) demonstrating correlation of NRP2 and Melan-A staining in serial tumor sections.

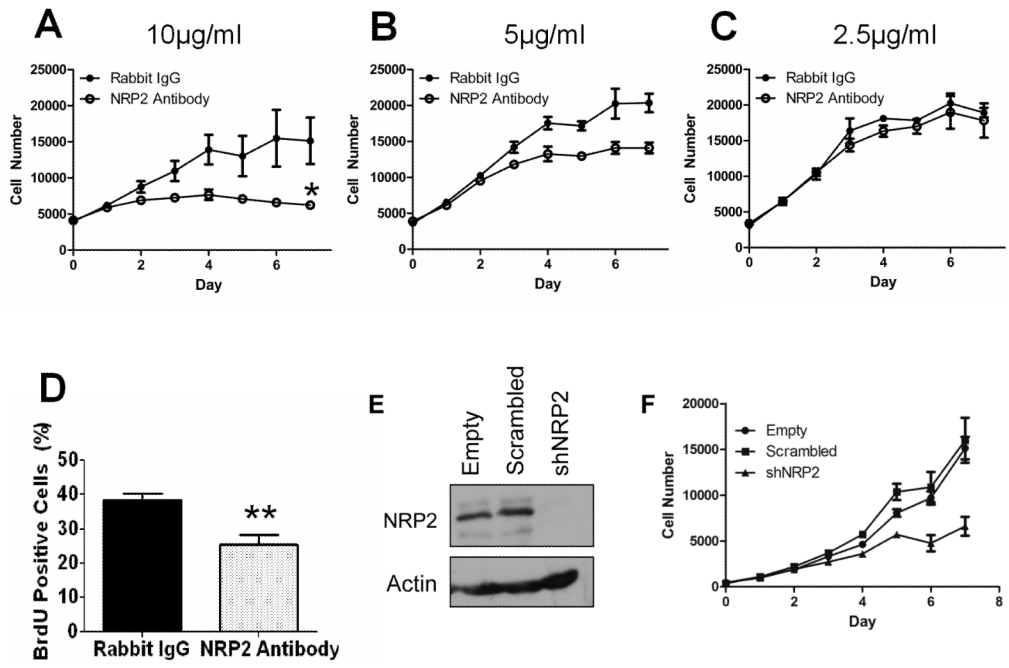

Figure 3. NRP2 Neutralizing Antibody and shRNA Knockdown Inhibits Metastatic Melanoma Cell Proliferation

(A–C) XTT Proliferation assay for GFP-1205Lu metastatic melanoma cells in the presence of 10ug/ml (A), 5ug/ml (B) or 2.5ug/ml (C) normal rabbit IgG (open circle) or rabbit polyclonal NRP2 antibody (closed circle).

(D) Quantification of BrdU incorporation in GFP-1205Lu cells following 48 hours of treatment with 10ug/ml NRP2 neutralizing antibody versus control antibody.

(E) Western blot for NRP2 expression in 1205Lu cells following empty vector, scrambled vector, and NRP2 shRNA (shNRP2) lentiviral infection.

(F) XTT Proliferation assay for empty, scrambled, and shNRP2 infected 1205Lu cells in the presence of media with 1% serum.

*$p < 0.05$, **$p < 0.01$

Error bars represent standard deviation

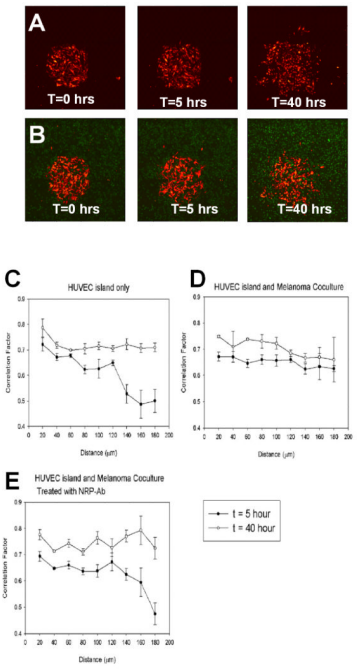

Figure 4. Analysis of Collective Cell Movements within HUVEC Colonies of DefinedInitial Geometry, Cell Number and Size (Method III) Suggests NRP2's Essential Role in Promotion of Cellular Patterning

(A) Expansion of a circular HUVEC alone colony in the absence of melanoma cells at T=0, 5, 40 hrs.

(B) Expansion of a circular HUVEC colony surrounded by a monolayer of GFP-1205Lu cells in the presence of NRP2-neutralizing antibody at T=0, 5, 40hrs.

(C–E) Quantitative analysis of collective cell movements from HUVEC colonies of defined geometry, cell number and size for HUVEC island alone (C), HUVEC Island and melanoma co-culture (D), and HUVEC Island and melanoma co-culture treated with NRP2-neutralizing antibody (E). Three independent co-culture experiments were performed for each condition. The error bars represent the standard error of the mean.

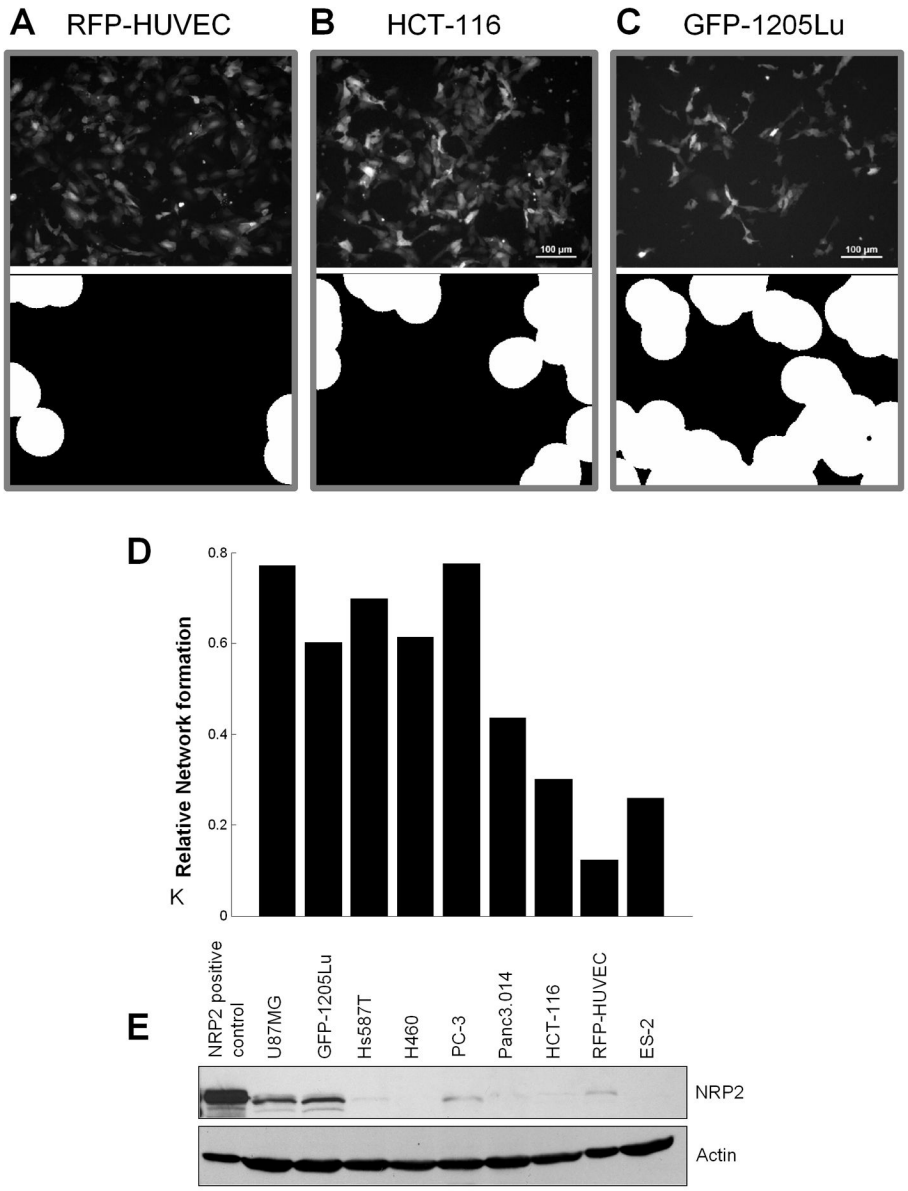

Figure 5. Cell-cell communications with different tumor cell types induces variable degree of HUVECs patterning

(A–C) Patternings of RFP-HUVECs co-cultured with different tumor cell lines were obtained following 48 hours of co-culture (top panel) and evaluated using the morphological analysis of HUVEC network formation (lower panel) described in Methods for (A) RFP-HUVECs alone, RFP-HUVEC's co-cultured with HCT-116 colon cancer cells (B), and RFP-HUVECs co-cultured with GFP-1205Lu melanoma cells (C).

(D) Quantification of the morphological analysis of HUVEC patterning induced by co-culture with various tumor cell lines vs. HUVEC alone.

(E) Western blot analysis of NRP2 expression in various tumor cell lines grown in heterotypic co-culture with RFP-HUVECs. The tumor cell lines used were: glioblastoma, U87MG; melanoma, GFP-1205Lu; breast cancer, Hs578T; non-small cell lung carcinoma, H460; prostate cancer, PC-3; pancreatic cancer, Panc3.014; colon cancer, HCT-116; ovarian cancer, ES-2.

Table 1

Melanoma-endothelial cell co-culture promotes the development of an invasive tumor phenotype

Gene Ontology Biological Process descriptions associated with transcripts altered in melanoma cells following coculture with HUVECs. Significant alterations are seen in genes associated with an aggressive tumor phenotype including altered cell migration, adhesion, and angiogenesis.

GO biological Process Description	p-value	Number of Transcripts	Number upregulated	Number Downregulated
Cell adhesion	8.94e-07	55	45	10
Regulation of cell-cell adhesion	0.015	4	4	0
Cell differentiation	0.0288	57	45	12
Negative regulation of cell differentiation	0.0214	9	8	1
DNA replication initiation	0.000971	6	0	6
Regulation of apoptosis	0.000703	33	22	11
Angiogenesis	0.00111	21	19	2
Regulation of cell migration	0.00744	12	12	0
Cell proliferation	0.000397	52	26	26
ECM organization	0.000268	9	8	1
Intercellular junction	0.0436	10	10	0

Table 2

Gene expression profiling data for the top 30 genes upregulated in melanoma cells following co-culture with HUVECs

A complete list of all gene expression profiling data for melanoma cells and HUVECs can be found at the NCBI's Gene Expression Omnibus (GEO) repository under the series record GSE8699.

Probeset ID	Gene Title	Gene Symbol	Fold
216438_s_at	Thymosin, beta 4, X-linked	TMSB4X	36.67
205612_at	Multimerin 1	MMRN1	14.93
201859_at	Proteoglyan 1, secretory granule	PRG1	14.79
214841_at	Cornichon homolog 3(Drosophila)	CNIH3	9.13
1556499_s_at	Collagen, type I, alpha 1	COL1A1	8.94
1555623_at	DERP12 (dermal papilla derived protein 12)	DERP12	7.80
232113_at	Hypothetical gene supported by BX647608	---	7.16
225566_at	Neuropilin 2	NRP2	6.33
823_at	Chemokine (C_X3_C motif) ligand 1	CX3CL1	6.31
226158_at	Kelch-like 24 (Drosophila)	KLHL24	6.21
207147_at	Distal-less homeo box 2	DLX2	5.95
230538_at	rai-like protein	RALP	5.73
212706_at	RAS p21 protein activator 4	RASA4	5.71
201667_at	Gap junction protein, alpha 1, 43kDa (connexin 43)	GJA1	5.65
201438_at	Collagen, type VI, alpha 3	COL6A3	5.61
237169_at	Tenascin C (hexabrachion)	TNC	5.49
227020_at	Yippee-like 2 (Drosophila)	YPEL2	5.47
213413_at	Stoned B-like factor	SBLF	5.46
203238_s_at	Notch homolog 3 (Drosophila)	NOTCH3	5.42
201858_s_at	Proteoglycan 1, secretory granule	PRG1	5.10
209071_s_at	Regulator of G-protein signaling 5	RGS5	5.01
202112_at	von Willebrand factor	VWF	4.98
238067_at	FLJ20298 protein	FLJ20298	4.89
225728_at	Importin 9	IPO9	4.82
44783_s_at	Hairy/enchancer-of-split related with YRPW motif 1	HEY1	4.78
226436_at	Ras association (RalGDS/AF-6) domain family 4	RASSF4	4.75
232797_at	Integrin, alpha V	ITGAV	4.72
231779_at	Interleukin_1 receptor-associated kinase 2	IRAK2	4.60